SLAC-3
UC-28, Particle Accelerators and
High-Voltage Machines
UC-34, Physics
TID-4500

SHOWER DEVELOPMENT AND HEATING IN THE WAVEGUIDE STRUCTURE WITH AN 800 MEV ELECTRON BEAM

July 1962

by

J. K. Cobb and J. J. Muray
Stanford Linear Accelerator Center

Technical Report
Prepared Under
Contract AT(04-3)-400
for the USAEC
San Francisco Operations Office

Printed in USA. Price $1.00. Available from the Office of Technical Services, Department of Commerce, Washington 25, D.C.

TABLE OF CONTENTS

LIST OF FIGURES

Page

I. INTRODUCTION

In a previous report[1] estimates were made of the axial and radial temperature gradients in the accelerator structure of the Stanford two-mile accelerator if a fraction of the electron beam were to strike the structure. Since the heating in the accelerator structure is actually a measure of the amount of energy absorbed by the structure, it would be expected that a temperature measurement along the axis would give some information about the axial shower development and perhaps about the radial development, in addition to providing information about the heat conduction properties of the waveguide.

In this report we will describe the results of such a measurement made on the Mark III accelerator using an 800 Mev electron beam. (Appended as a final section are the results of a separate experimental study of the thermal characteristics of a single cavity with high power arc heating, performed to investigate heat conduction properties at high temperature.)

II. EXPERIMENTAL APPARATUS

The experimental apparatus for this experiment consisted of a section of disk-loaded copper accelerator structure two feet long, with ten probe-type thermistors inserted into the first ten disks from one end (front end) in such a way that the sensing elements were 1 mm from the inside edge of the irises. (See Fig. 1.) Three additional thermistors (11, 12, and 13) were attached to the outer skin of the waveguide section. The structure was cooled with water by 1/4-inch copper tubing which was soldered to the skin of the section. A bridge circuit was used so that the resistance of each thermistor could be measured. (See Fig. 2.) The thermistors used for this measurement were VECO 34 A 3.

---

[1] J.J. Muray, "Shower Development and Heating in the Accelerating Structure of a 50-Bev Linear Electron Accelerator," M Report No. 276, Stanford Linear Accelerator Center, Stanford University, Stanford, California, September 1961.

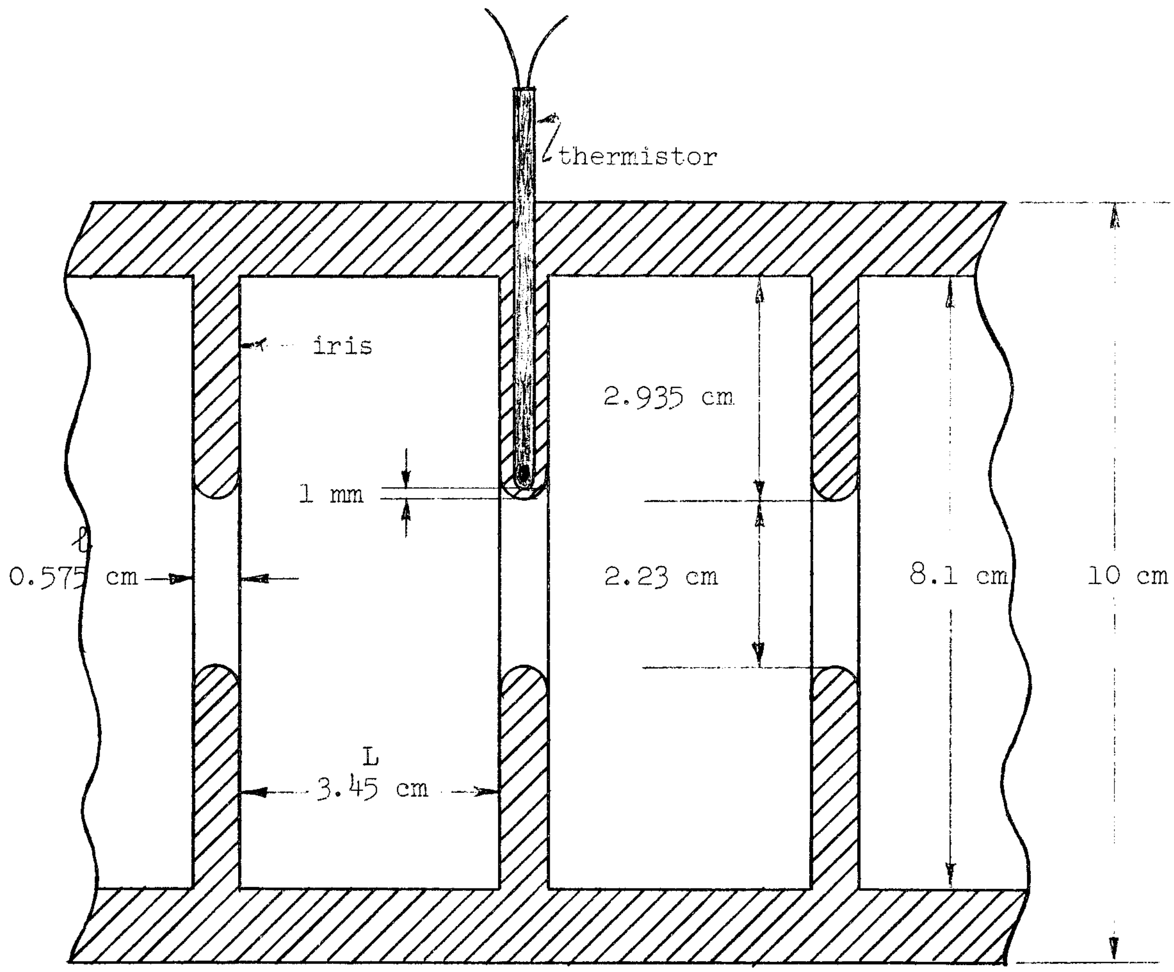

FIG. 1--Cross-section view of the accelerator structure showing the placement of probe-type thermistors.

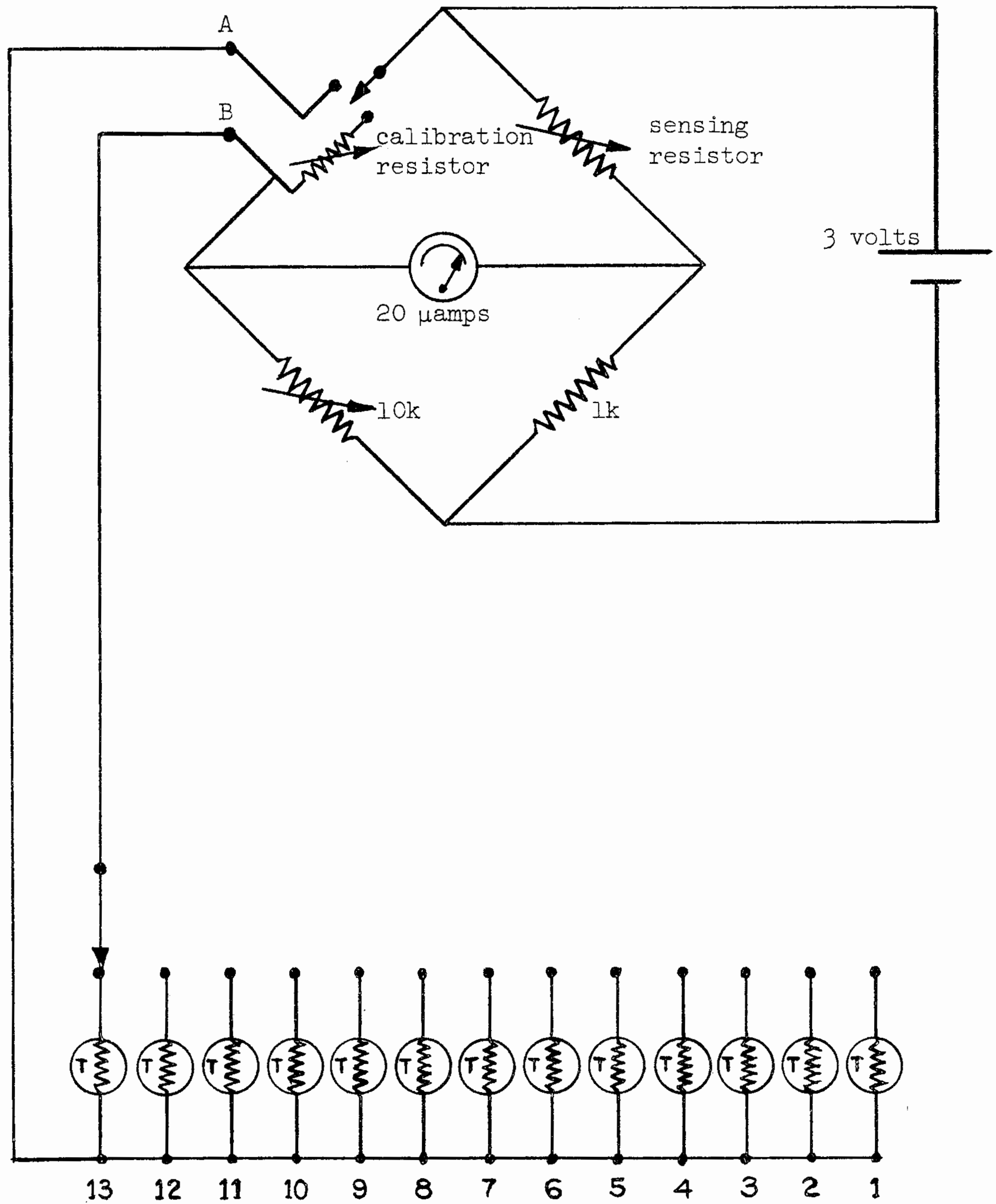

FIG. 2--Thermistor resistance measuring bridge circuit.

III. THERMAL CHARACTERISTICS OF A THERMISTOR

The resistance of a thermistor is generally given by the relation

$$R = R_s \exp \beta \left[\left(\frac{1}{T} - \frac{1}{T_s}\right)\right]$$

where R_s is the resistance at the absolute temperature T_s, T is the instantaneous thermistor temperature, and β is a positive constant representative of the material from which the thermistor is manufactured. The temperature coefficient of resistance is, by definition,

$$\eta(T) = \frac{1}{R_o}\left(\frac{dR_o}{dT}\right) = -\frac{\beta}{T^2}$$

For the thermistors used in this measurement, η is approximately - 3.8 per degree at 20 degrees. When the thermistor is heated to a temperature T and then permitted to cool, the rate of cooling is found to be proportional to the instantaneous temperature difference $T - T_x$, T_x being the temperature of surroundings. If c is the heat capacity of the thermistor, the transfer equation is

$$\frac{dT}{dt} = -\frac{k}{c}(T - Tx)$$

The parameter k is defined as the dissipation factor. The time constant τ is defined as

$$\tau = \frac{c}{k}$$

which is about two seconds for the bead type thermistor which was used here.

IV. SYSTEM THERMAL CHARACTERISTICS

The other important characteristic time of the system is the heat time constant of the whole two-foot accelerator section. To estimate this time constant, one may assume that the heat flow is limited to the radial direction in the waveguide and $T(r,t)$ satisfies the heat conduction equation

$$K\nabla^2 T = - S + \rho C \frac{\partial T}{\partial t} \qquad (1)$$

where

K is the thermal conductivity

S is the heat source strength in watts per cm^3

ρ is the density of the copper

and

C is the specific heat.

If T_o is the equilibrium temperature, then Eq. (1) may be simplified using

$$T(r,t) = T_o(r) + T_1(r,t)$$

where T_o is defined by

$$K\nabla^2 T_o = - S \qquad (2)$$

and T_1 satisfies the following equation

$$\nabla^2 T_1 = \frac{\partial^2 T_1}{\partial r^2} + \frac{1}{r}\frac{\partial T_1}{\partial r} = \frac{\rho C}{K}\frac{\partial T_1}{\partial t} \qquad (3)$$

The solution of Eq. (3) can be written in the form

$$T_1(r,t) = \sum_n R_n(r)e^{-\gamma_n t} \tag{4}$$

where R_n is function of the radial position and $\gamma_n > 0$. If the power is turned on at $t = 0$ and when the temperature is T_i then

$$T_1(r,0) = T_i - T = \sum_n R_n(r)$$

and from Eqs. (2), (3) and (4),

$$\left[\frac{\partial T_1}{\partial t}\right]_{t=0} = \frac{K}{\rho C} \nabla^2 T_1(r,0) = \frac{S}{\rho C} = -\sum_n \gamma_n R_n$$

and

$$\frac{\sum_n \gamma_n R_n}{\sum_n R_n} = - \frac{S}{\rho C T_1(r,0)} \tag{5}$$

Equation (5) gives a weighted average of the γ_n; it is reasonable that the negative reciprocal

$$t_o = \frac{\rho C}{S} T_1(r,0) \tag{6}$$

be regarded as a time constant of the system because this is the time which is required for the temperature to rise from T_i to T_o if the system is thermally insulated. In our case the time constant can be estimated from Eq.(6), using 1020 watts for the heater power and 2000 cm^3 for the system volume.

$$t_o = \frac{\rho C}{S} T \approx \frac{8.93 \times 9.3 \times 10^{-2}}{0.5} 300 \approx 500 \text{ sec}$$

To check the calculation, measurements were made of how the temperature of the structure behaved as a function of time as the structure was heated at a fixed heater power and with a fixed coolant flow. At the start, resistance of each thermistor was recorded with the structure at equilibrium with the cooling water. At $t = 0$ the heating element was switched on and a timer was started. The resistance of each thermistor and the time of measurement were recorded as the structure heated. Five thermistors were used in this part of the experiment, three on the inside of the structure and two on the skin. From this data, information on how the inside and outside temperatures differed as a function of time was determined. The result of this measurement is depicted in Fig. 3.

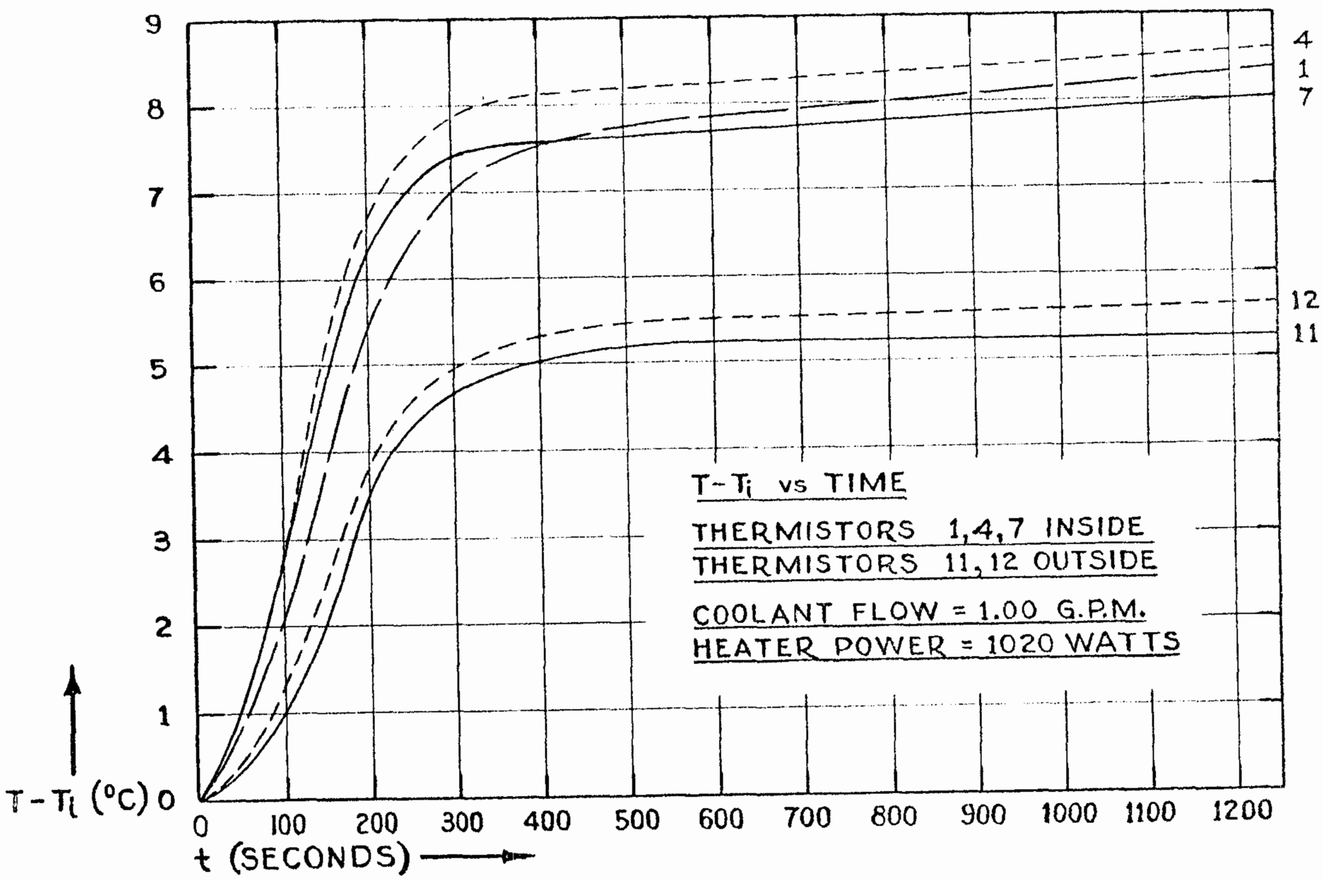

FIG. 3--Temperature increase with time.

The experimental value of $\tau \approx 300$ seconds is in very good agreement with the calculated one. Therefore, to reach thermal equilibrium in the system, the required time must be longer than the time constant of the thermistors as well as the time constant of the whole waveguide.

V. THERMISTOR CALIBRATION

For the thermistor calibration, a heating element of the same length as the accelerator section was inserted into the center hole of the section to provide heating on the inside. Provision was made to control both the temperature and the flow rate of water circulating through the cooling tubes. Provision was also made to read voltage and amperage in the heater rod to find the power expended.

It was first necessary to calculate the rate of change of resistance as a function of temperature for each thermistor. This was done by enclosing the entire waveguide structure in a box constructed of high thermal resistance material (in this case, heavy pasteboard) and, with temperature-regulated water circulating through the cooling coils, letting the entire structure come to equilibrium temperature. (Equilibrium temperature is that where the temperature of the water in equals the temperature of the water out equals the temperature of the inside of the box as indicated by mercury thermometers.) The resistance of each thermistor was recorded. This procedure was repeated for a higher temperature and from this data the quantity $\Delta R/\Delta T$ was calculated for each thermistor (see Fig. 4). Since the quantity $\Delta R/\Delta T$ is not constant for a large range of temperature, the calculation was made over a small range of temperature within the expected range of the experiment. This calculated value for $\Delta R/\Delta T$ was checked against a wide variation of temperature for one thermistor and the linear approximation was found to be a good one over the range of temperature expected in the experiment. Actual difference in the calculated value of $\Delta R/\Delta T$ for the two methods was found to be less than 3%.

The resistance measurements of the thermistors were converted to temperature changes in the following way. The resistance of each thermistor varies with temperature in an almost linear fashion for all reasonably small ($\Delta T < 15^{\circ}C$) changes of temperature in the operating range of

Thermistor	R(ohms) at $20.2^{\circ}C$	R(ohms) at $31.0^{\circ}C$	ΔR(ohms) over $\Delta T = 10.8^{\circ}C$	$\Delta R/\Delta T$ at $T_{mean} = 25.6^{\circ}C$	$-(\Delta T/\Delta R)$ at $T_{mean} = 25.6^{\circ}C$
1	3070	2020	- 1050	- 97.2	0.010288
2	3370	2220	- 1150	- 106.5	0.009389
3	3540	2320	- 1220	- 113.0	0.008849
4	3330	2190	- 1140	- 105.5	0.009478
5	3100	2040	- 1060	- 98.0	0.010204
6	3090	2030	- 1060	- 98.0	0.010204
7	3120	2030	- 1090	- 100.9	0.009910
8	3490	2280	- 1210	- 112.0	0.008928
9	3720	2410	- 1310	- 121.2	0.008250
10	3380	2190	- 1190	- 110.2	0.009074
11	3240	2170	- 1070	- 99.0	0.010101
12	3100	2060	- 1040	- 96.2	0.010395
13	3200	2110	- 1090	- 100.8	0.009920

Fig. 4--Table of thermistor calibration data.

the thermistor. In Table 1 the quantities $(\Delta R/\Delta T)_T$ were determined at $T = 25.6^{\circ}$, the mid-range of the calibration temperatures taken. In linear approximation the temperature difference as a function of resistance difference is given by the relation $(T - T_o) = (R - R_o)\ (\Delta T/\Delta R)$.

The next series of measurements consisted of finding out how each thermistor changed as a function of the power in the heating element for various flow rates. The power levels used were 100 watt steps from 0 to 1000 watts. The flow rates used were 0.25 gallons per minute, 0.5 gpm, 1.0 gpm and 1.5 gpm. Each measurement of thermistor resistance was made after the structure had achieved equilibrium with heater and cooling water flow.

Graphs of $(T - T_o)$ as a function of power, while water flow in the cooling coils was held constant, were made for each thermistor. (See Figs. 5 through 17.) These graphs pointed out a very important point regarding the structure: In addition to a large radial flow of heat there is present a smaller but not negligible axial flow introduced primarily by the design of the cooling coils.

For display and study of the axial flow, the quantity $T - T_o$ was graphed as a function of thermistor location for various heating conditions at various cooling rates. (See Figs. 18 through 21.)

In interpreting the curves of Figs. 5 through 21, note that Thermistor 1 was inside the structure at the input end, Thermistor 2 inside and next down from the input and so forth to Thermistor 10 which was inside and furthest from the input. Thermistors 11, 12 and 13 were on the skin of the section, starting at the input end.

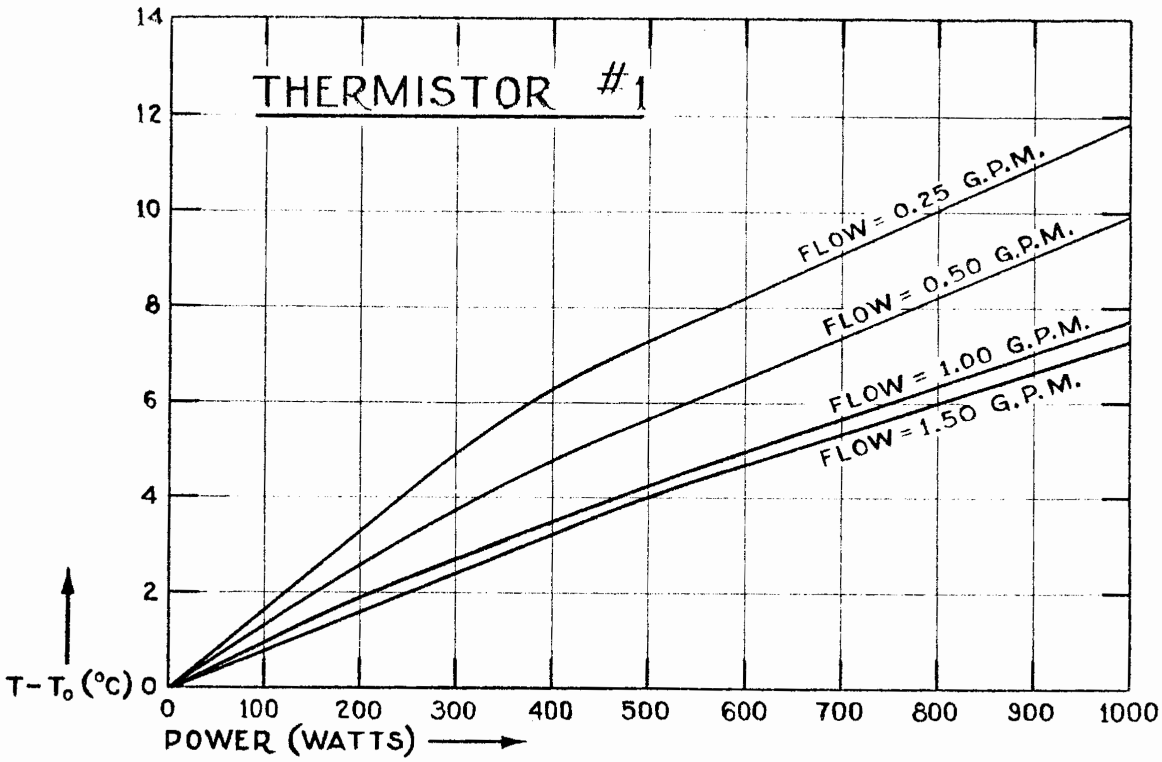

FIG. 5--Temperature rise vs heating power, Thermistor 1.

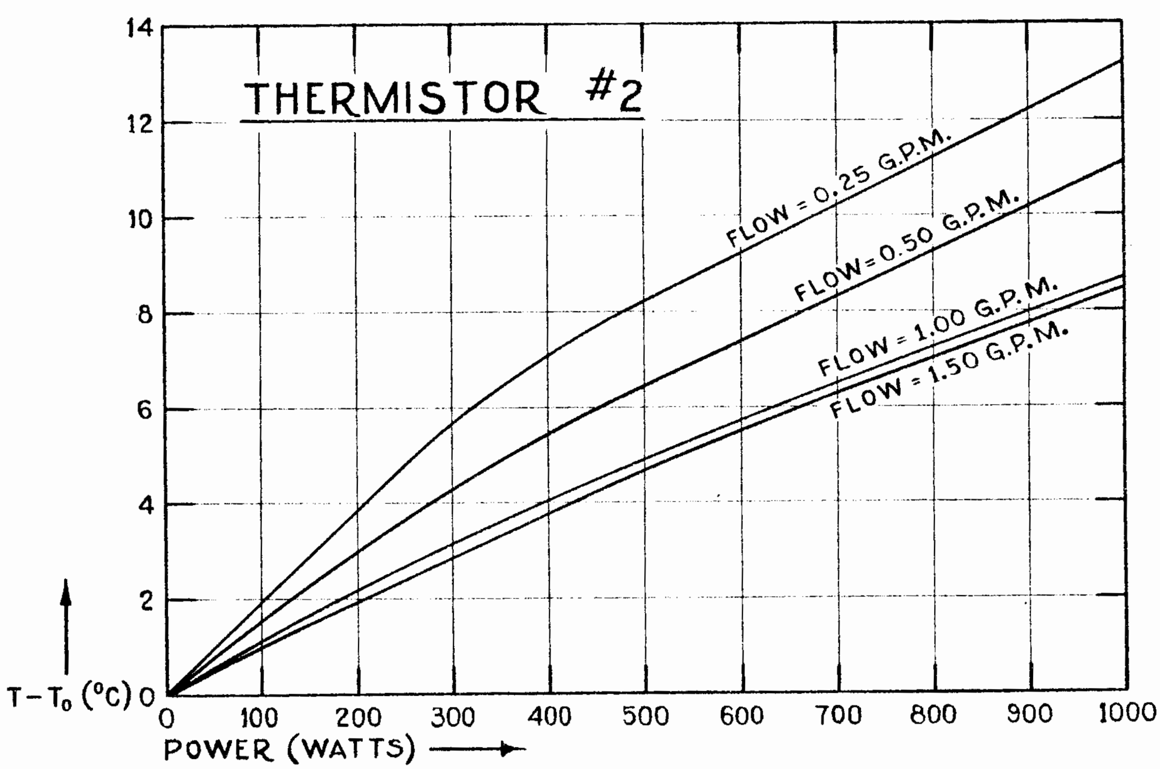

FIG. 6--Temperature rise vs heating power, Thermistor 2.

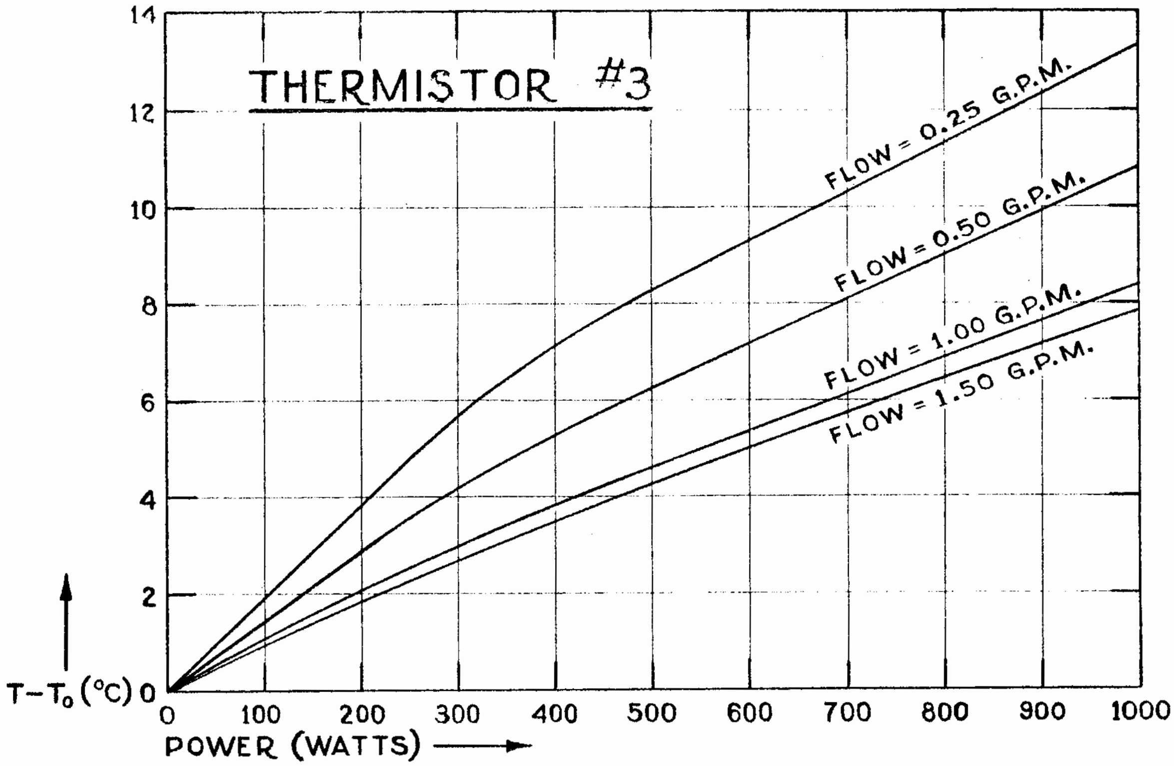

FIG. 7--Temperature rise vs heating power, Thermistor 3.

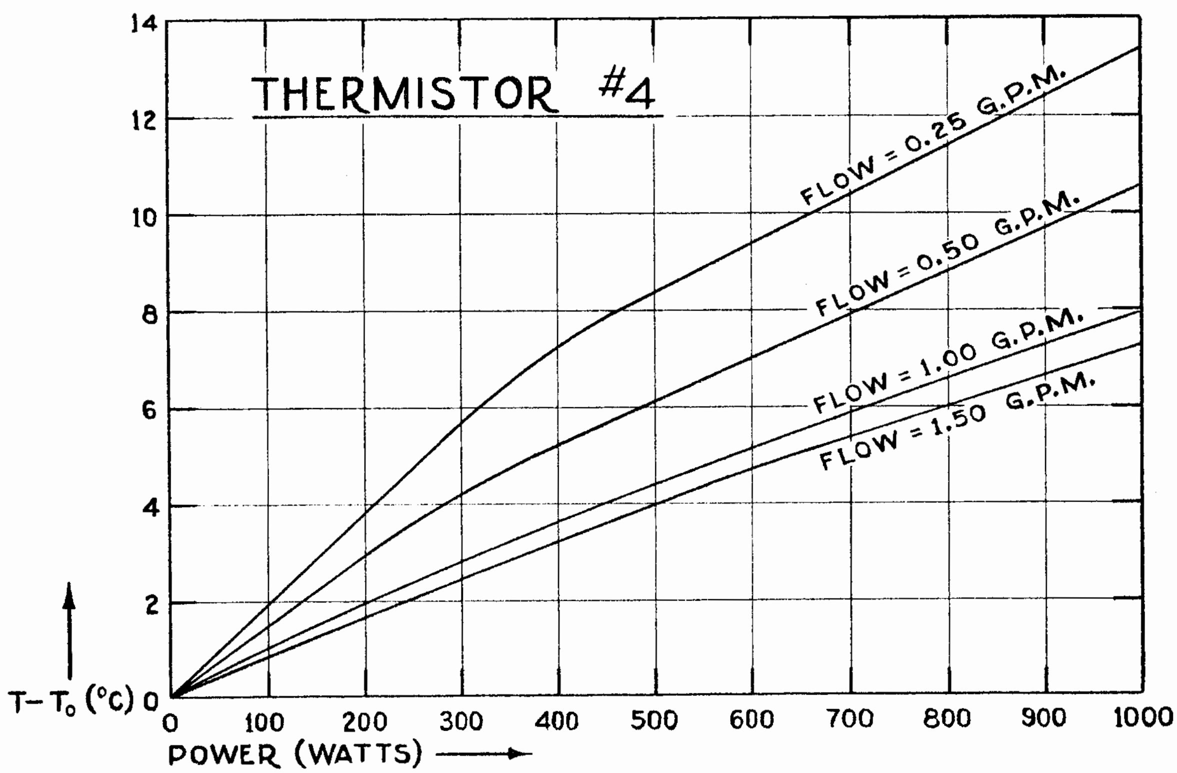

FIG. 8--Temperature rise vs heating power, Thermistor 4.

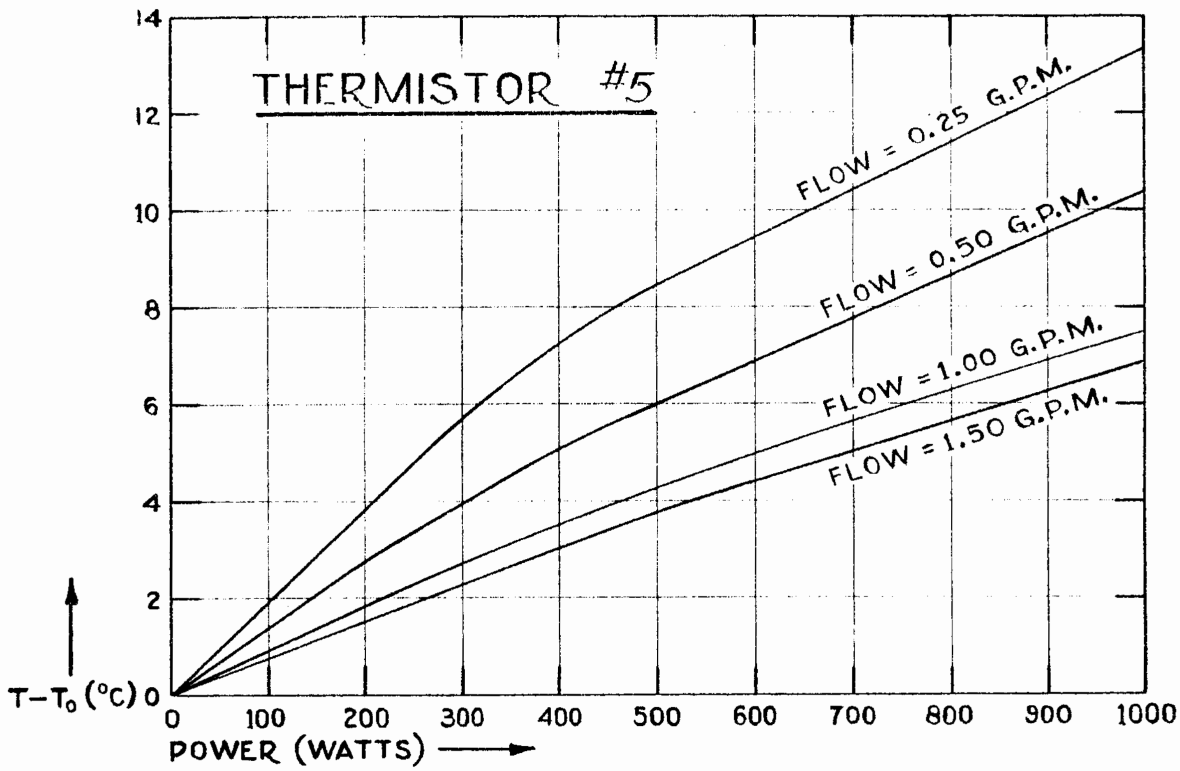

FIG. 9--Temperature rise vs heating power, Thermistor 5.

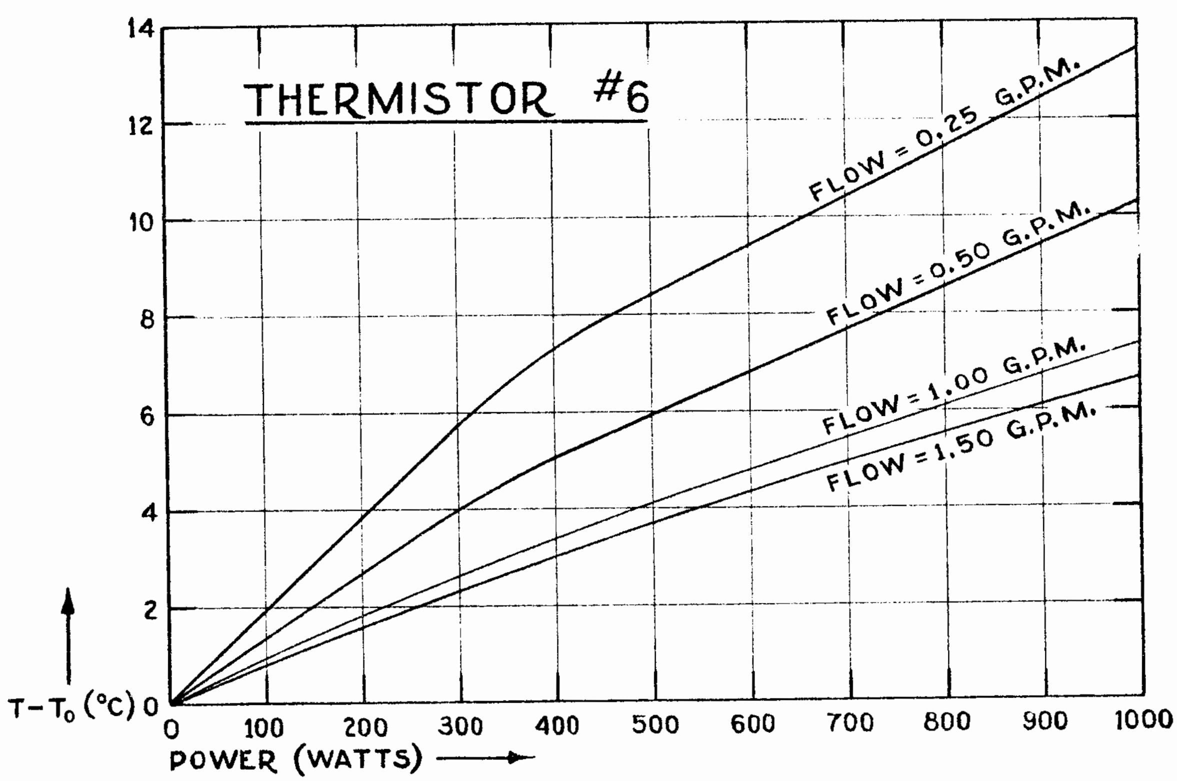

FIG. 10--Temperature rise vs heating power, Thermistor 6.

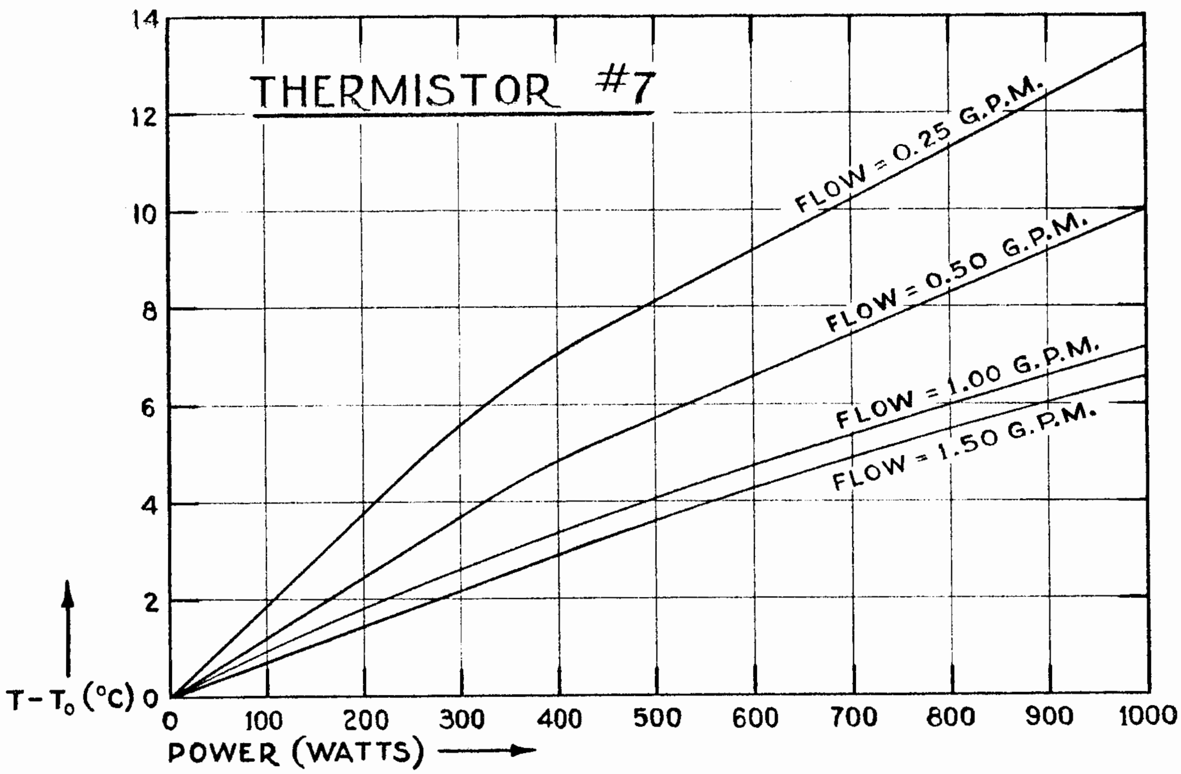

FIG. 11--Temperature rise vs heating power, Thermistor 7.

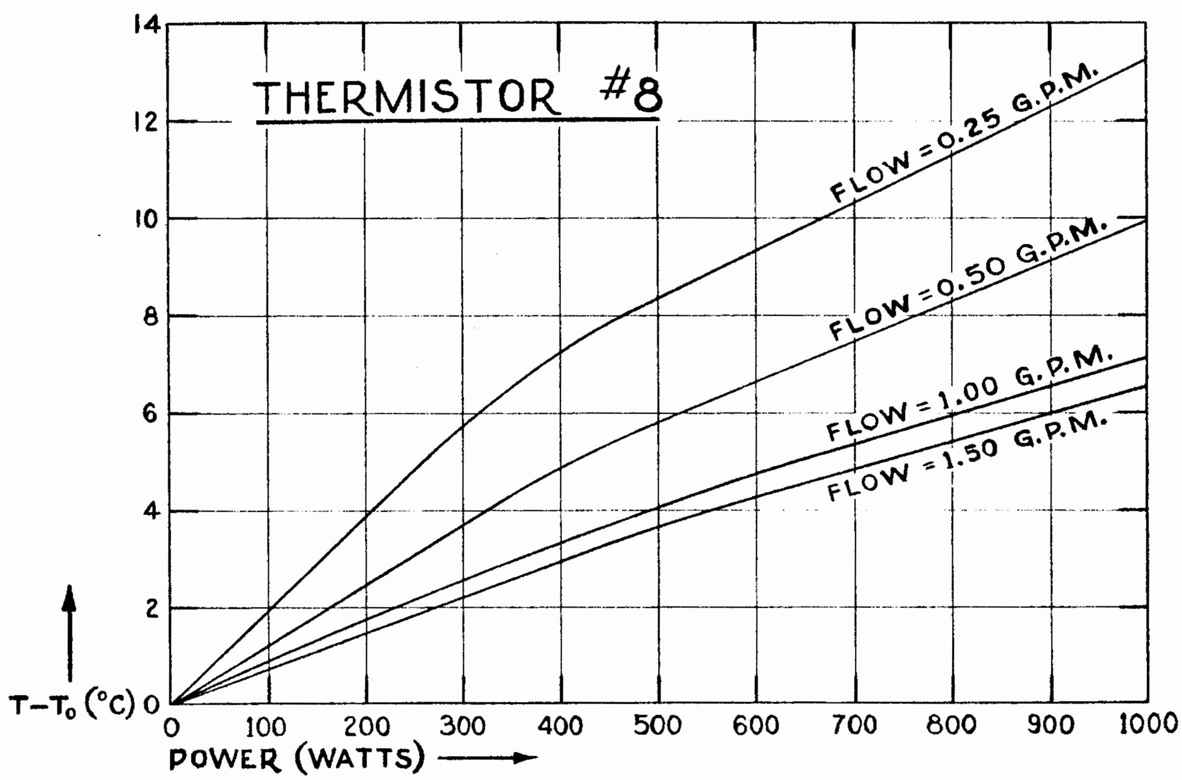

FIG. 12--Temperature rise vs heating power, Thermistor 8.

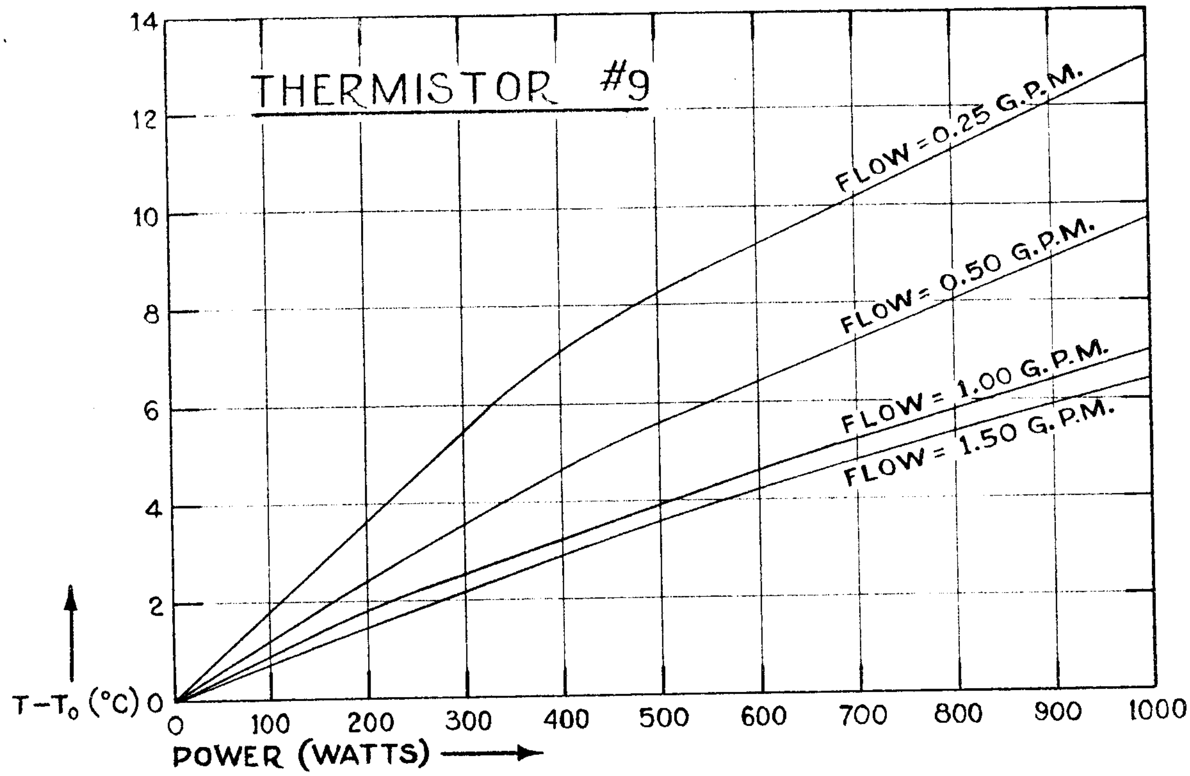

FIG. 13--Temperature rise vs heating power, Thermistor 9.

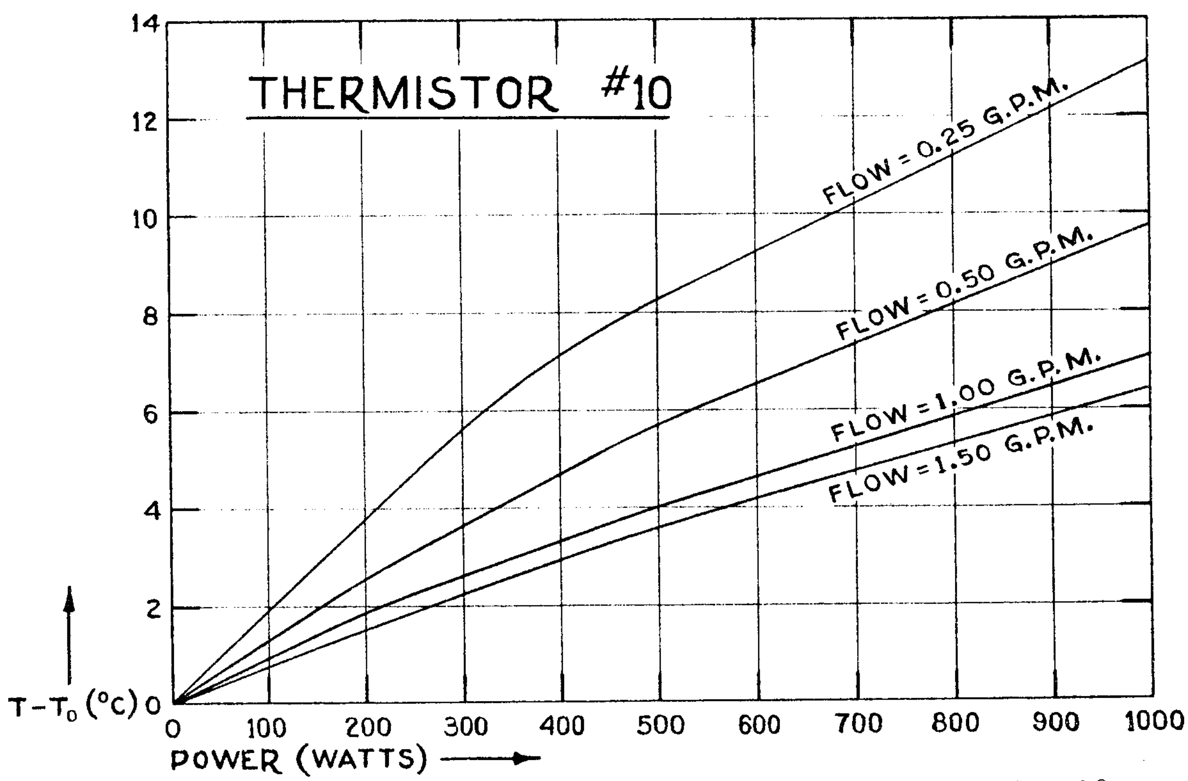

FIG. 14--Temperature rise vs heating power, Thermistor 10.

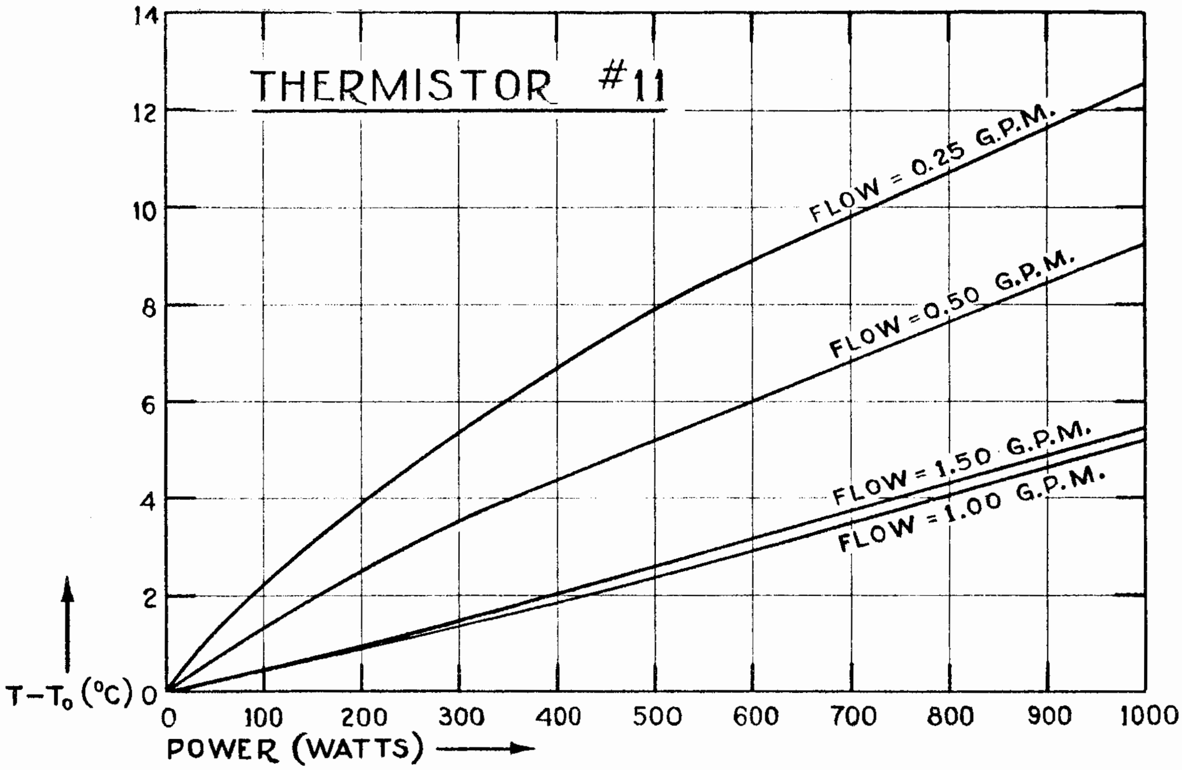

FIG. 15--Temperature rise vs heating power, Thermistor 11.

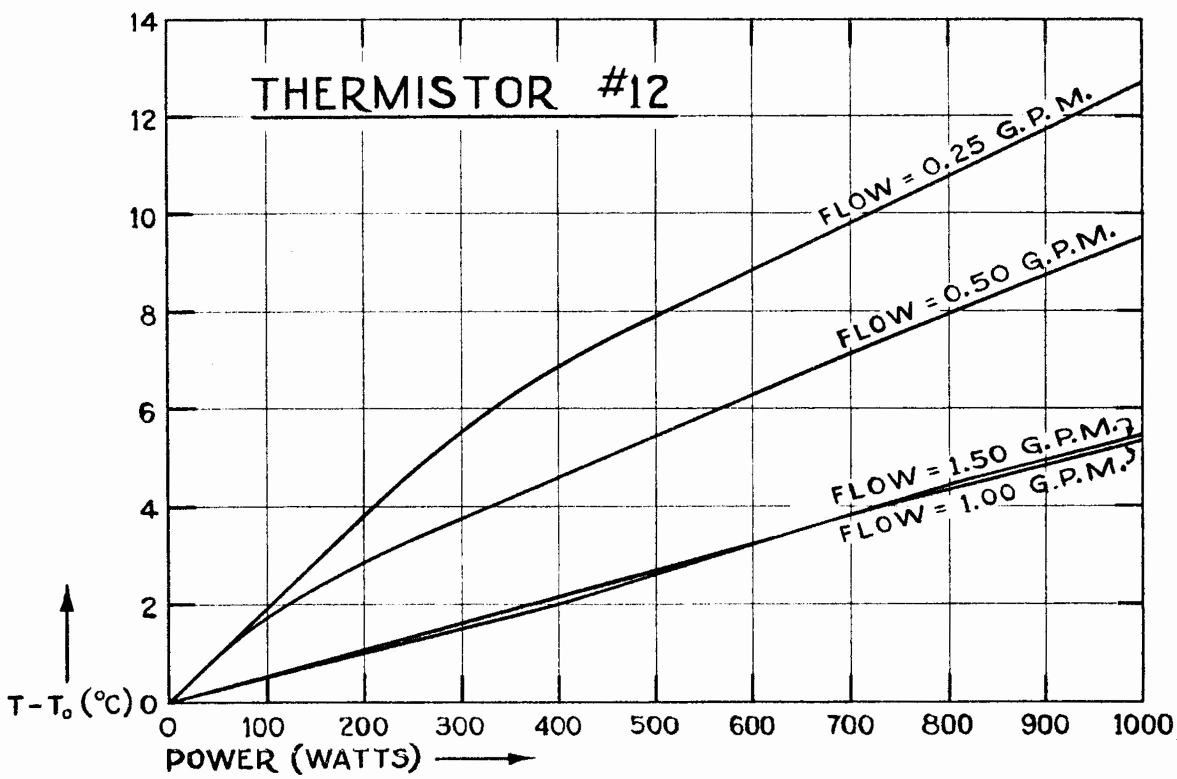

FIG. 16--Temperature rise vs heating power, Thermistor 12.

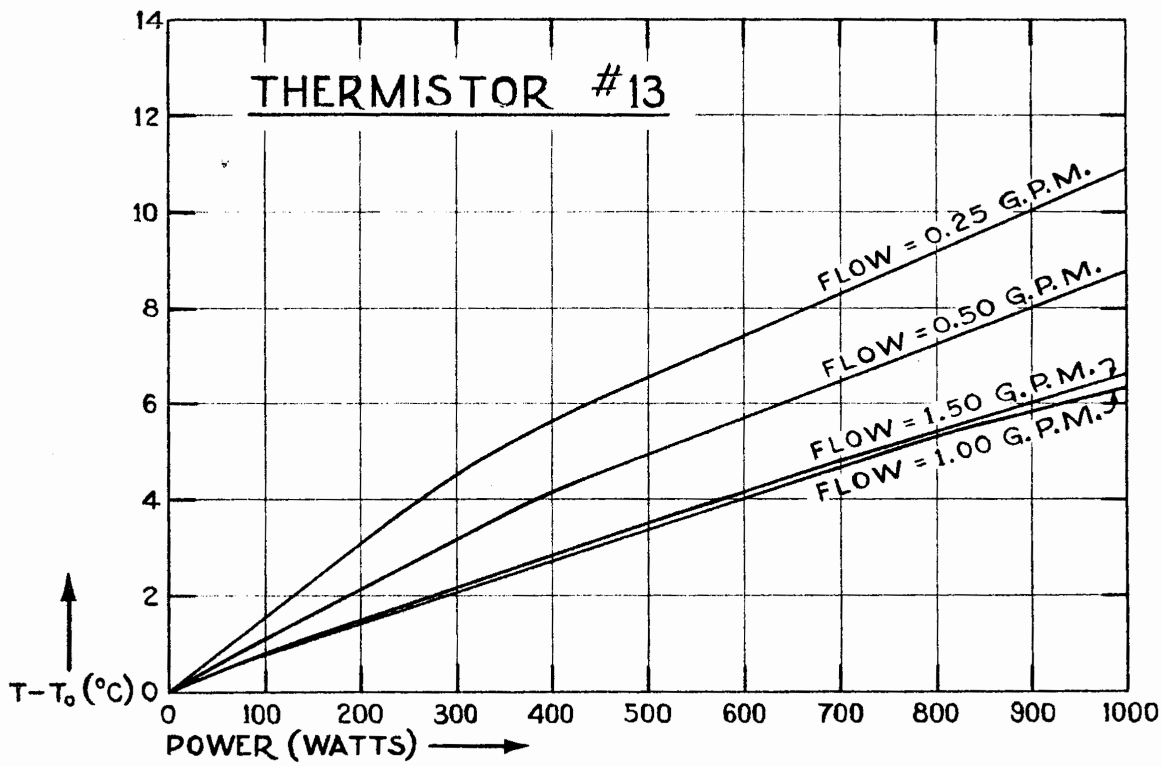

FIG. 17--Temperature rise vs heating power, Thermistor 13.

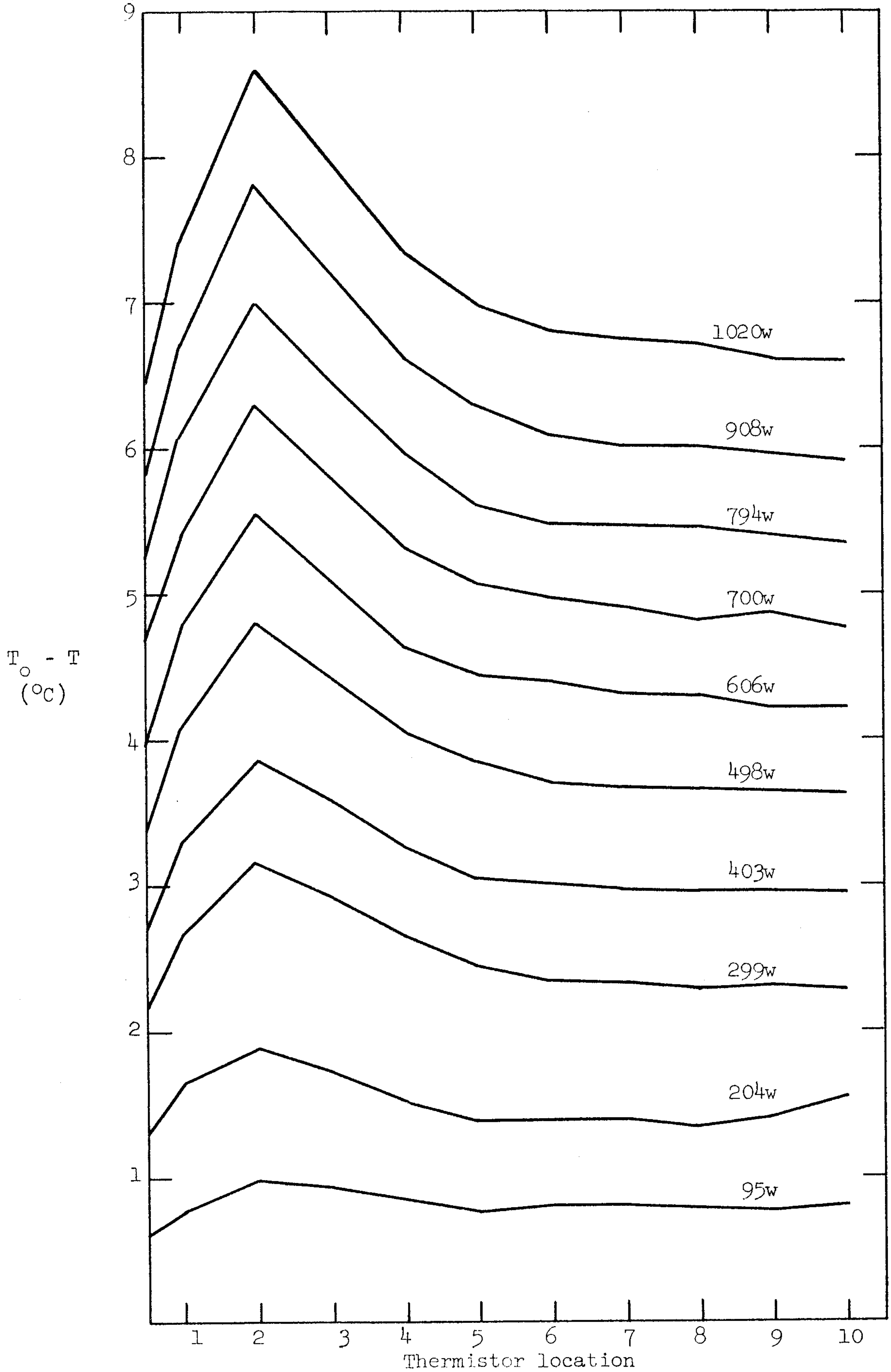

FIG. 18--Comparison of reaction of thermistors as a function of thermistor location. Structure is centrally heated. Coolant temperature is 24.0^oC. Coolant flow is 1.5 gpm.

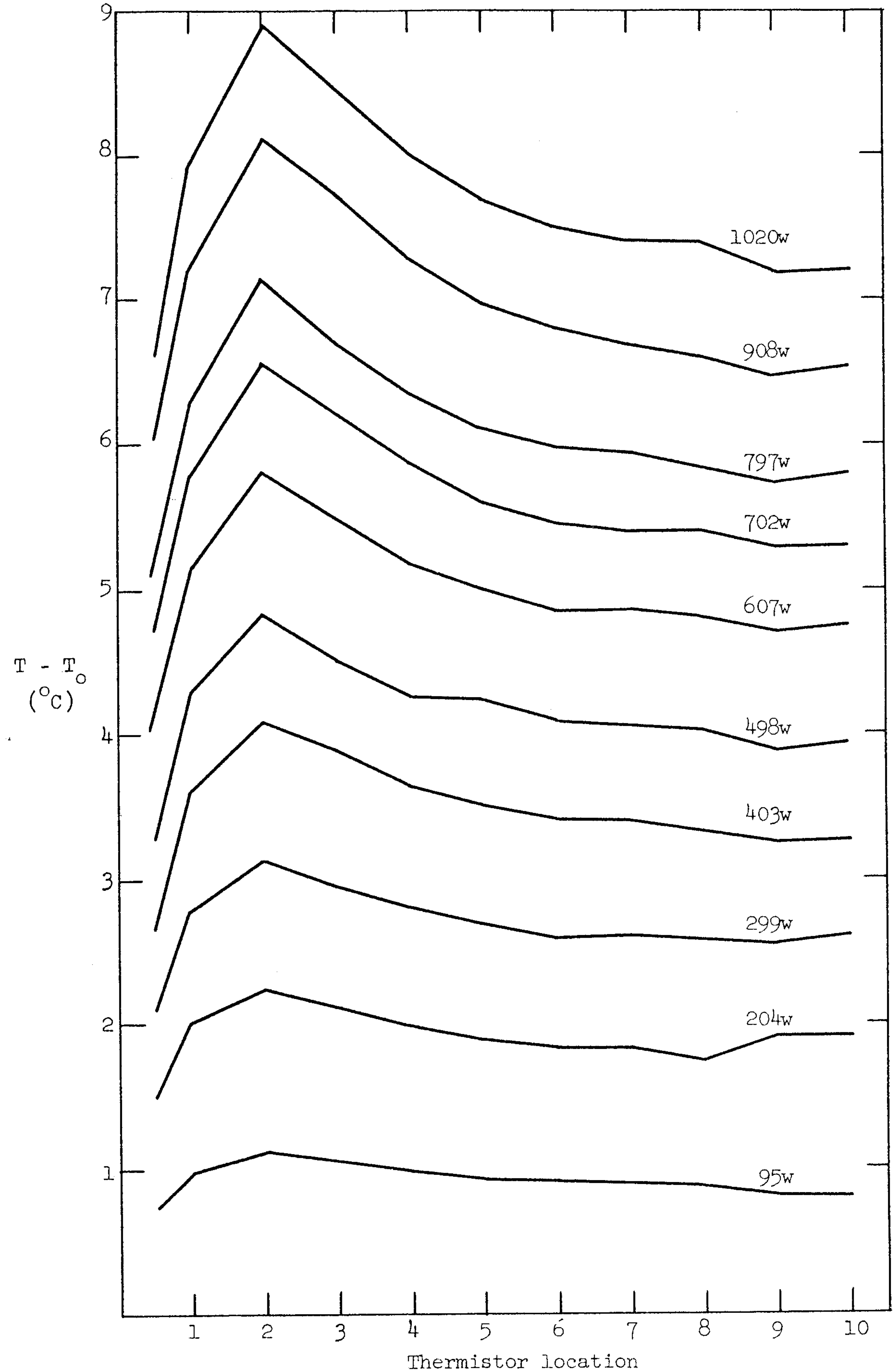

FIG. 19--Comparison of reaction of thermistors as a function of thermistor location. Structure is centrally heated. Coolant temperature is 24.0°C. Coolant flow is 1.0 gpm.

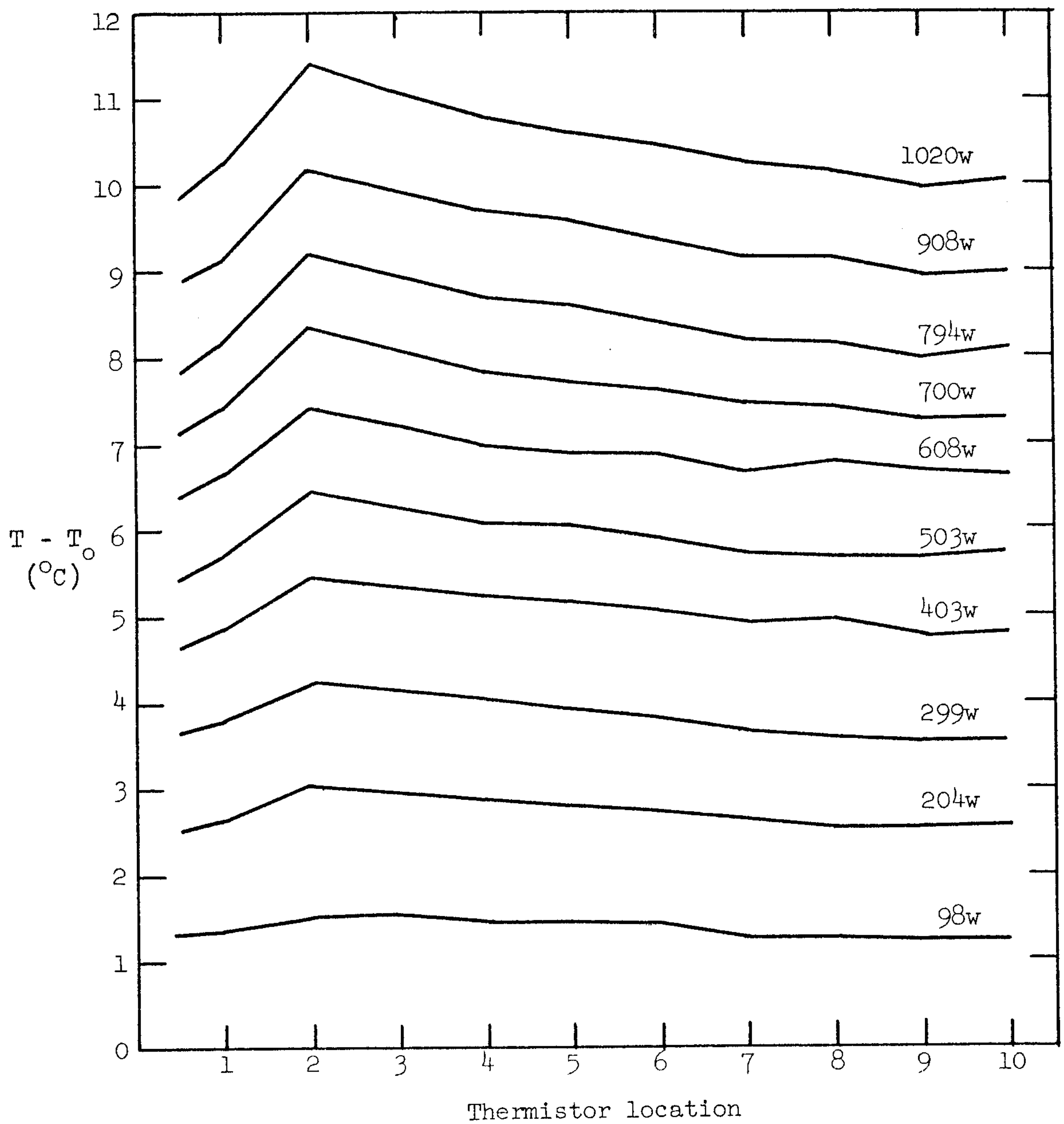

FIG. 20--Comparison of reaction of thermistors as a function of thermistor location. Structure is centrally heated. Coolant temperature is 24.0°C. Coolant flow is 0.5 gpm.

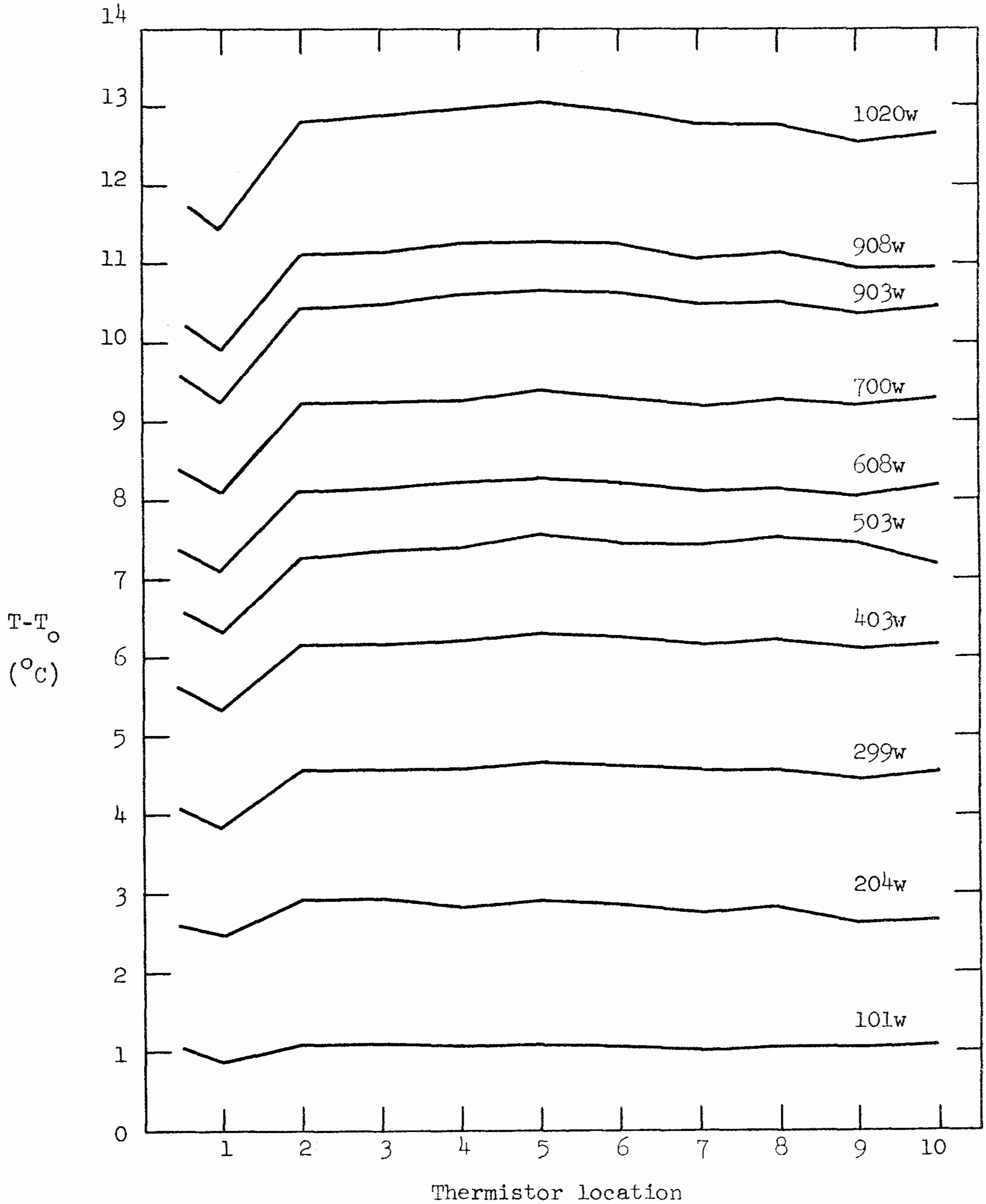

FIG. 21--Comparison of reaction of thermistors as a function of thermistor location. Structure is centrally heated. Coolant temperature is 24.0° C. Coolant flow is 0.25 gpm.

VI. EXPERIMENTAL RESULTS OF THE HEATING OF THE ACCELERATOR SECTION BY AN 800 MEV ELECTRON BEAM

A beam of electrons from the Mark III Linear Accelerator was allowed to impinge on the first disk of the structure and the thermistors were used to measure the temperature change of the waveguide structure as a function of the axial position. Figure 22 shows the position of the incoming beam as indicated on a glass slide attached to the structure. Figure 23 shows the uniform clouding of a similar slide located at the exit end of the accelerator section.

Two different beam currents were used, and a water flow of 1.0 gallon per minute was maintained throughout the run. The temperature difference between the hot (beam impinging) values and the cold (no beam) values was obtained by applying the resistance change of the thermistors to their individual characteristics and obtaining the equivalent temperature change.

The thermistor readings were taken after thermal equilibrium was established in the structure, ten minutes after the beam-on time. (This time must be longer than any characteristic time constant of the system.) The beam current was measured by a secondary-emission monitor which had an efficiency of 10%. Taking into account that the fraction of the beam which actually hit the first iris was $\approx \frac{10}{13}$ of the total beam, the actual average beam currents were:

$$I_1 = 0.554\ \mu\text{amp}$$

$$I_2 = 1.308\ \mu\text{amp}$$

and the beam energy measured by a calibrated deflection magnet was 800 Mev.

The temperature difference between the inside and outside surfaces of the first waveguide disk can be calculated from the following formula[2]

$$\Delta T = 0.088\ \frac{n\alpha r_1 \ell \log\left(\frac{r_2}{r_1}\right)}{\lambda \ell} \qquad (7)$$

[2]Muray, <u>op. cit.</u>

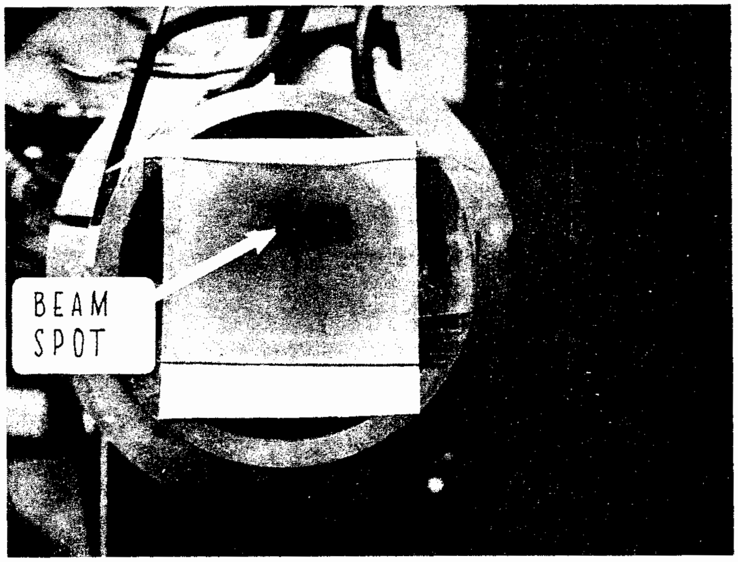

FIG. 22--Glass slide attached to the entrance to the structure showing the incoming beam.

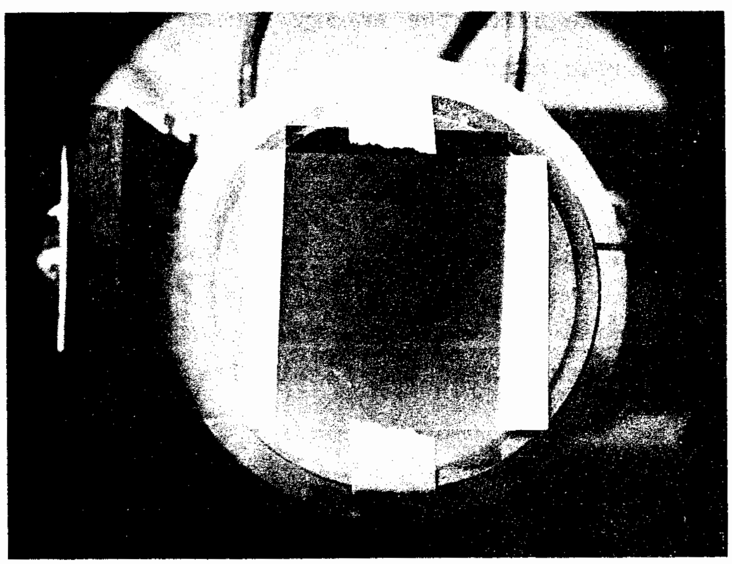

FIG. 23--Glass slide across the exit of the structure showing uniform clouding.

where r_2 and r_1 are the outside and inside diameters of the disk respectively and

ℓ = the thickness of the disk in cm.

λ = the heat conduction coefficient = 0.94.

n = the number of electrons per second which strike the disk.

$\alpha = \frac{t}{r_1}$ where t is the beam spot thickness.

(In this measurement $\alpha \approx 10^\circ$.)

The calculated temperature difference due to the beam heating is $1.9^\circ/\mu amp$ at 1 Bev when $\alpha = 360^\circ$. Then in this case with the two beam currents

$$I_1 = 0.554\ \mu amp \qquad \Delta T_1 = \frac{1.9^\circ}{\mu amp} \times 0.554\ \mu amp \times 36 = 37.9^\circ C$$

$$I_2 = 1.308\ \mu amp \qquad \Delta T_2 = \frac{1.9^\circ}{\mu amp} \times 1.308\ \mu amp \times 36 = 89.47^\circ C$$

A correction must be made for the energy, which was 800 Mev rather than 1 Bev. Taking a linear approximation,

$$\Delta T_1 = 37.9^\circ C \times 0.80 = 30.3^\circ C$$

$$\Delta T_2 = 89.5^\circ C \times 0.80 = 71.6^\circ C$$

The observed temperature increase in the first disk was

$$\Delta T_1(\text{meas}) = 29.0^\circ C$$

$$\Delta T_2(\text{meas}) = 73.0^\circ C$$

The agreement with the calculation is within 1.9%.

Temperature rise in the succeeding disks (following the first) cannot be calculated because α is unknown in those disks. It is extremely difficult to calculate the radial development of the shower caused by the following effects in the disks:

(1) Multiple Coulomb scattering.
(2) Compton scattering of γ rays.
(3) Angular separation in pair production.
(4) Angular separation of the bremsstrahlung gamma-ray from the incident electron.

However, from the measured temperature rise, it is possible to estimate α and with this the radial development of the shower. But to do this the measured temperature difference must be corrected for the "water heating effect." The "water heating effect" is the result of the cooling water having been heated at the leading part of the accelerator section and causing the succeeding disks (which the water is supposed to cool) to have a higher temperature than the beam heating alone would cause.

The calculated power expended in the structure was 30 watts per disk. There were 18 disks in the structure so the total power expended was 540 watts. From Fig. 19, using this value of power, the water heating correction factor can be obtained. This water heating correction factor was subtracted from the experimental ΔT. For the first disk, Thermistor 1, this factor is not subtracted since the cooling water was not preheated by the structure.

The temperature difference corrected for the water heating effect, as a function at the thermistor location, is plotted in Fig. 24. With these temperature difference values, the angle of divergence α as a function of radiation length in the waveguide section can be calculated from Eq. (7). This value of α, compared with the angular spread due to the multiple Coulomb scattering, is plotted against the radiation length in Fig. 25. Because $r_2 - r_1$ is decreasing as a function of the axial position, the heat conduction formula, Eq. (7), overestimates α. This graph cannot be extended beyond 2.2 radiation lengths because at 2.2 radiation lengths the shower is a maximum.

The real value of the angular spread lies between α and the angle $\bar{\theta}$ for multiple Coulomb scattering.

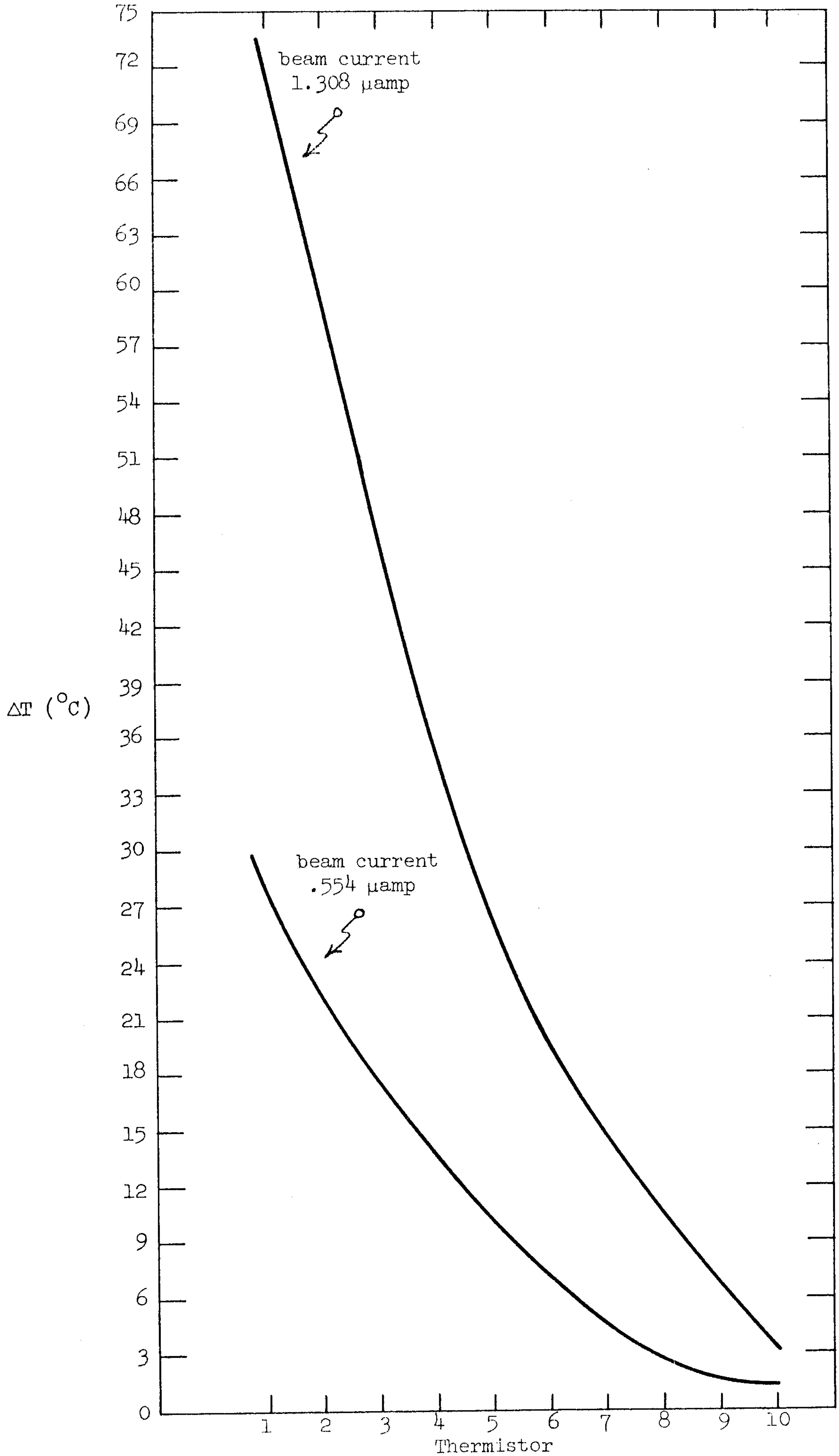

FIG. 24--Temperature difference, corrected for water heating, as a function of thermistor location.

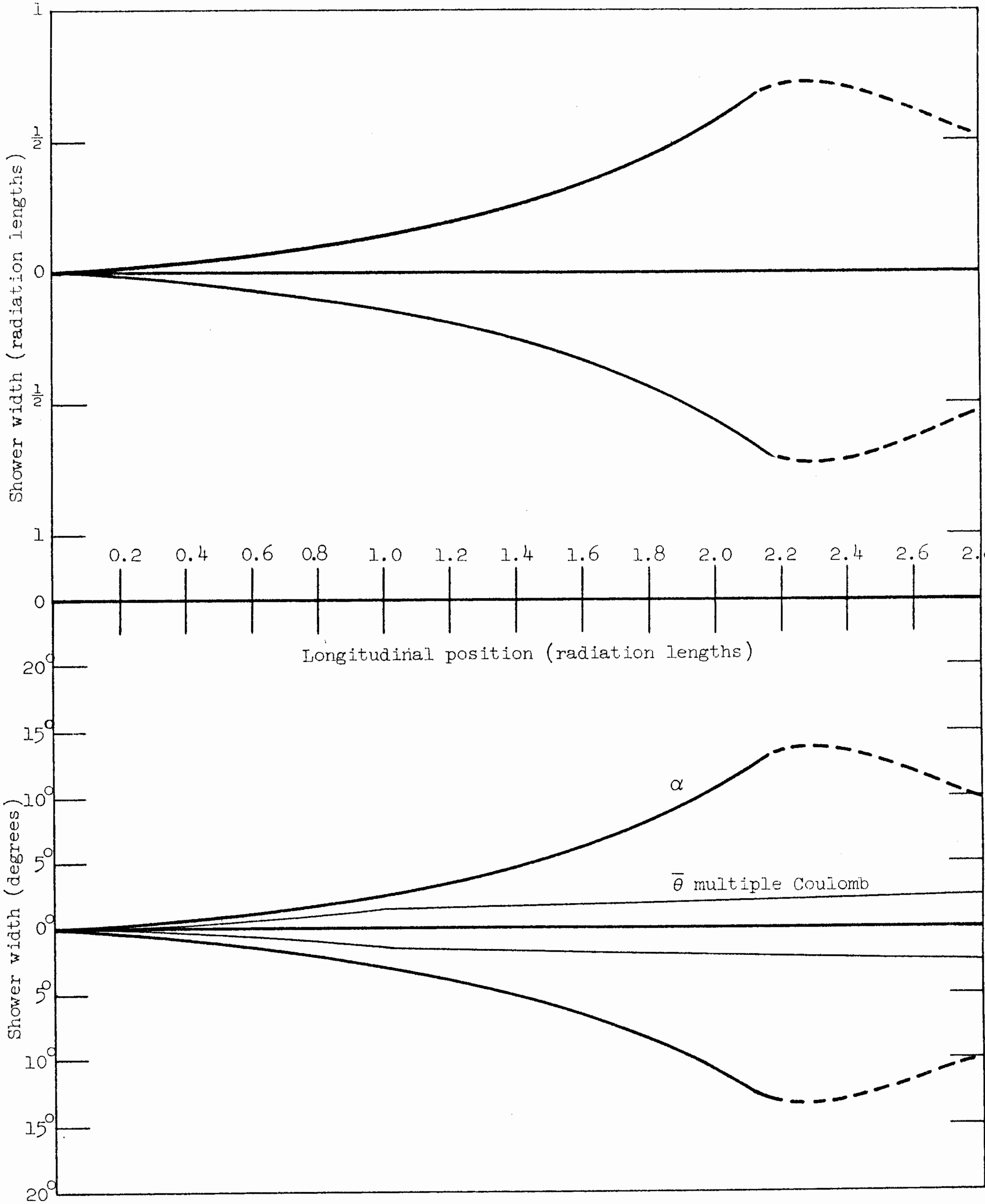

FIG. 25--Angle of divergence (α) compared with angular spread due to multiple Coulomb scattering ($\overline{\theta}$) plotted against radiation length.

VII. STUDY OF THE THERMAL CHARACTERISTICS OF A SINGLE CAVITY WITH HIGH POWER ARC HEATING

We calculated earlier that the temperature rise in the hottest disk in the waveguide structure should be about $3200^{\circ}K$ if the total beam of 60 μa at 50 Bev should hit the structure. To study the heat conduction property of the waveguide at high temperatures, an experiment was constructed to determine ΔT as function of the heating power. The heating element was a high intensity metal arc between a tungsten electrode and the copper cavity disk in inert gas atmosphere. The experimental setup is shown in Fig. 26. The heat distribution in this type of metal arc is generally sharper than Gaussian[3] and its half width is the order of one centimeter. The plasma temperature in the arc is the order of $10,000^{\circ}K$ and the anode power is greater than 75% of the total arc power.

The data which was collected consisted of the temperature difference between the incoming cooling water and the cavity skin. This was observed by a pair of thermocouples; the quantity observed was the potential difference between the outputs. These potentials were converted to temperature differences by use of the iron-constantan thermocouple tables. The arc power was determined by simultaneous readings of arc amperage and arc voltage when the thermocouple potential had reached its steady value. Figure 27 shows the temperature difference between the incoming water and cavity skin as a function of power into the center of the cavity for various water cooling rates. These curves were made under the assumption that 75% of the arc power was deposited into the cavity. From the heat conduction formula,[4]

$$\Delta T = 0.088 \frac{N \log_{10}\left(r_2/r_1\right)}{\lambda \ell}$$

[3]O. H. Nestor, J. Appl. Phys., May 1962, 1638.

[4]Muray, op. cit.

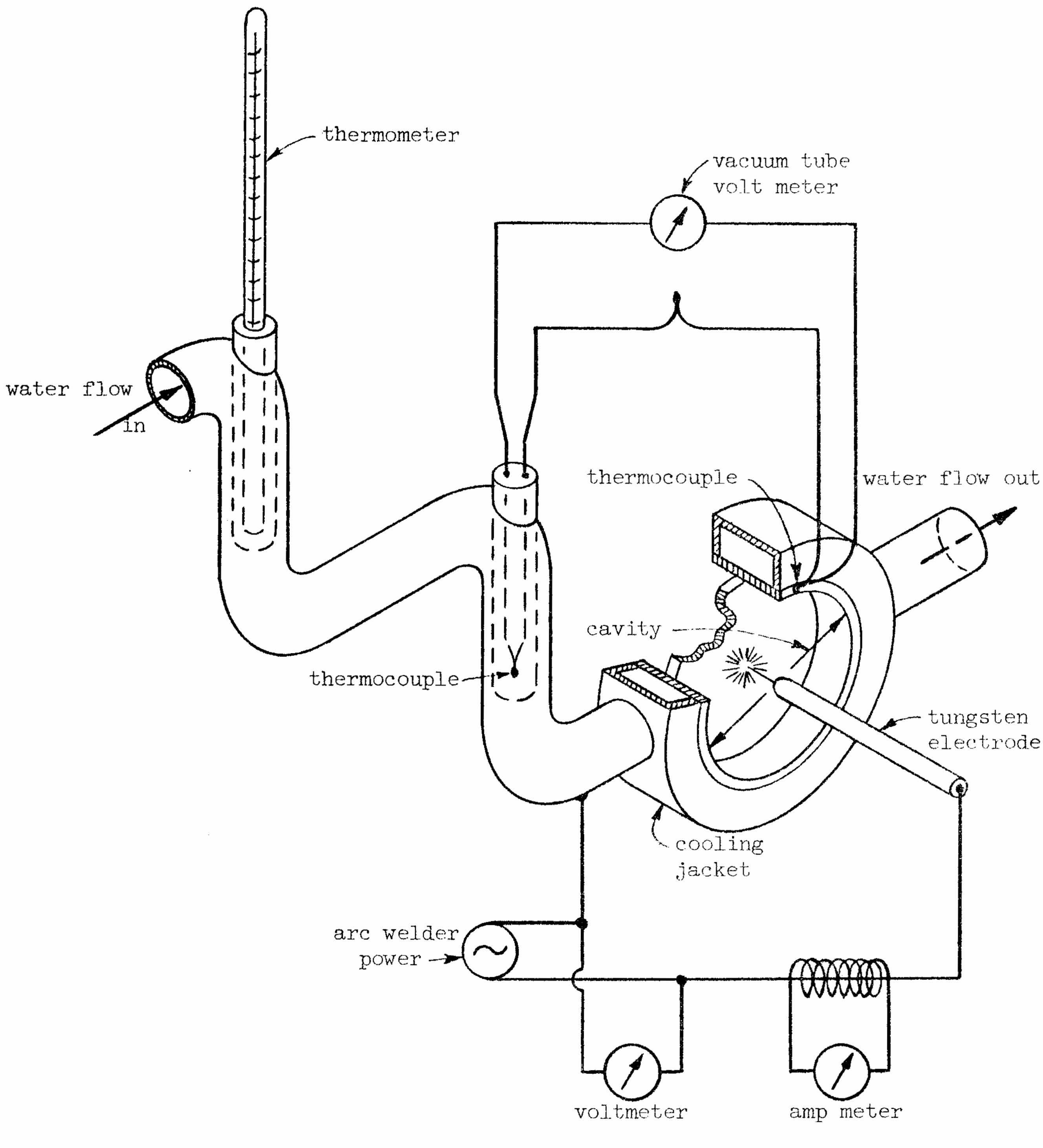

FIG. 26--Experimental arrangement for high power arc heating.

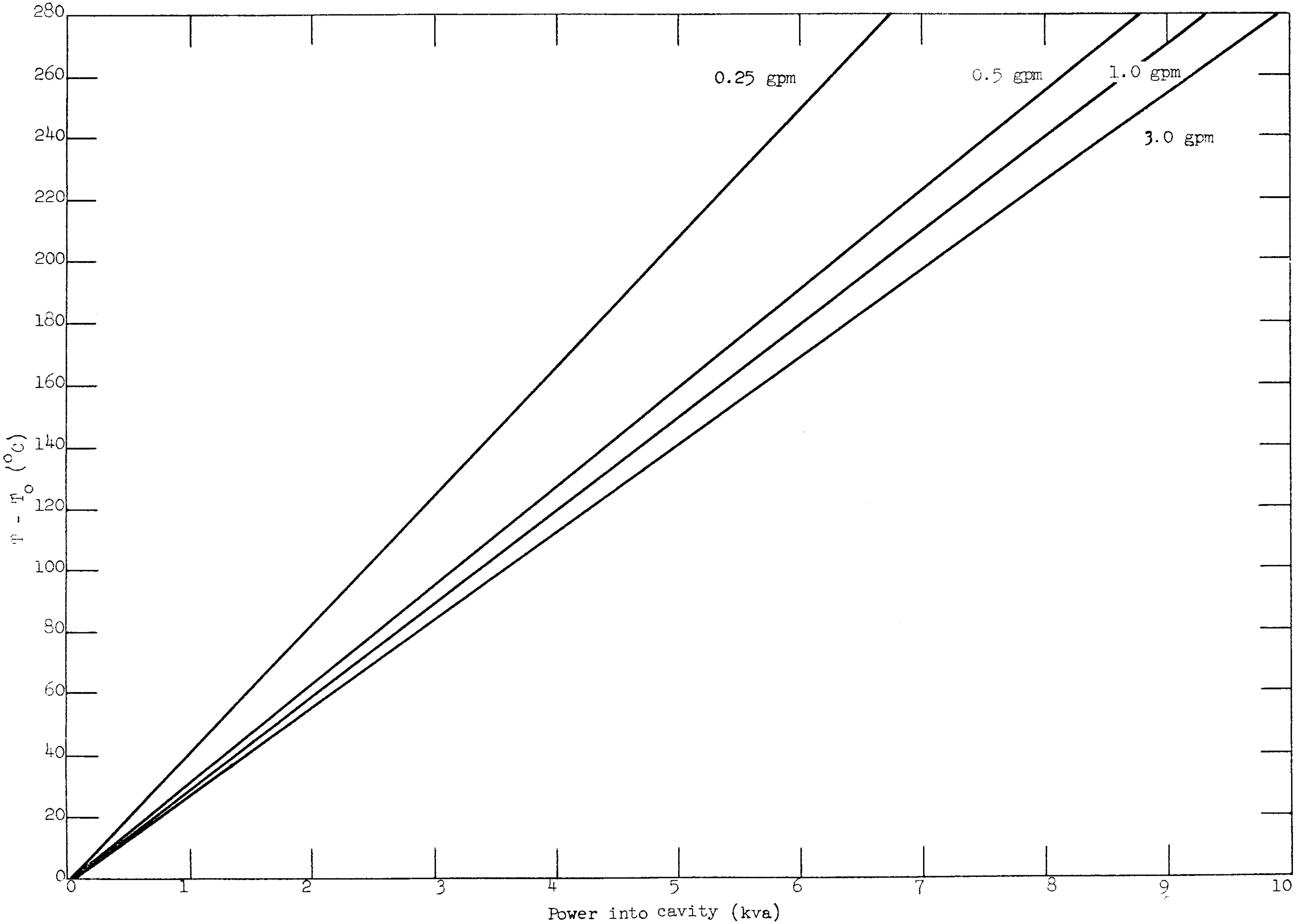

FIG.27--Temperature difference between the incoming water and the cavity skin versus power into the cavity.

where

N = the total dissipated power (watts)

r_2 and r_1 = outside and inside diameters of the iris

ℓ = the thickness of the disk

λ = the heat conduction coefficient
= 0.94 Cal/cm°C/sec

the temperature difference between the arc spot and the outer skin can be calculated. In our case r_2 is 10 cm, r_1 is 0.1 cm and ℓ is 0.64 cm.

The temperature difference ΔT between the arc spot and the outside cavity skin has been calculated and plotted as a function of the power into the cavity in Fig. 28. Also in Fig. 28 is plotted the temperature difference between the arc spot and the incoming water as a function of the power in, when the cooling water flow is 1 gallon per minute.

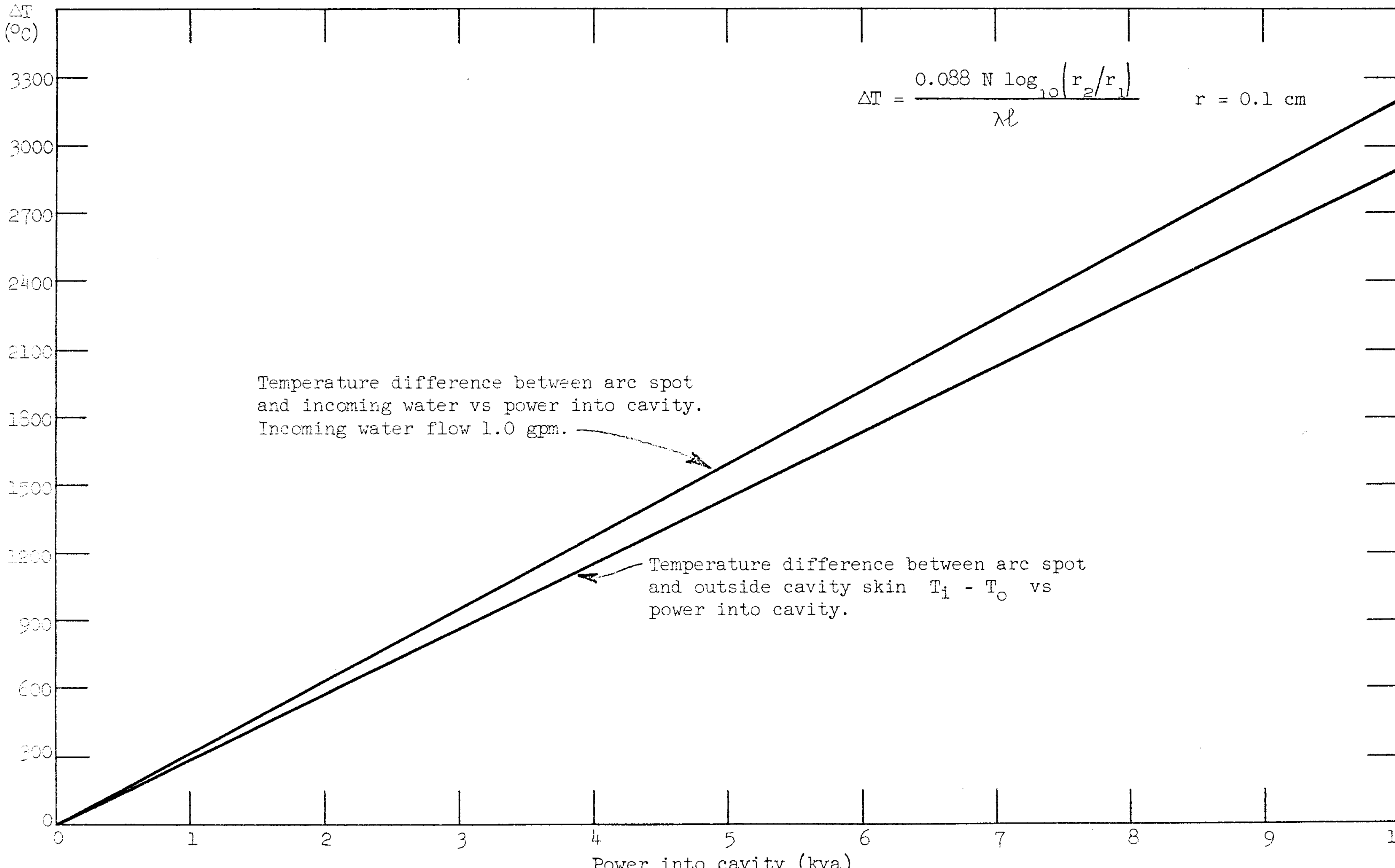

FIG. 28--Arc spot temperature differences versus power into the cavity.